JNeurosci
THE JOURNAL OF NEUROSCIENCE

Research Articles | Behavioral/Cognitive

Opioid-glutamate interactions modulate intrinsically rewarded communication in European starlings

https://doi.org/10.1523/JNEUROSCI.1131-26.2026

Received: 6 July 2026
Revised: 21 October 2026
Accepted: 27 October 2026

Copyright © 2026 the authors

This Early Release article has been peer reviewed and accepted, but has not been through the composition and copyediting processes.The final version may differ slightly in style or formatting and will contain links to any extended data.

Alerts: Sign up at www.jneurosci.org/alerts to receive customized email alerts when the fully formatted version of this article is published.

Title: Opioid-glutamate interactions modulate intrinsically rewarded communication in European starlings

Abbreviated Title: Opioid-glutamate interactions and birdsong

Author names and affiliations, including postal codes:

Changjiu Zhao, Ruoxi Fu, Grace E. Preston, Lauren V. Riters

Department of Biology, University of Wisconsin-Madison, Madison, WI 53706, USA

Corresponding author email address: LVRiters@wisc.edu

Number of pages: 37

Number of figures: 11

Number of tables: 0

Number of words for abstract: 250

Number of words for introduction: 642

Number of words for discussion: 1494

Conflict of interest statement: The authors declare no competing financial interests.

Acknowledgments: We gratefully acknowledge funding from the National Institutes of Health R21 MH134420 to LVR. We thank Jeffrey Alexander and Michelle Muhasky for animal care. Generative AI tools were used to assist with language editing and to improve the clarity and logical flow of the manuscript; all scientific contents and interpretations were reviewed and approved by the authors.

JNeurosci Accepted Manuscript

Abstract

Affiliative, non-sexual vocal communication is essential for social learning and bonding, yet relatively little is known about its neural bases. Past research on songbirds demonstrates that song produced in affiliative, non-sexual flocks correlates positively with a bird's intrinsic reward state, and the link between song and reward is regulated by mu opioid receptors (MORs) in the medial preoptic area (MPOA). RNAseq studies also reveal a strong positive association between affiliative song and glutamatergic gene expression in MPOA, with NMDA receptor 1 (GRIN1) and glutamate receptor scaffolding protein (Shank2) correlating strongly with affiliative singing. In male European starlings we tested the hypothesis that MOR–glutamate interactions in the MPOA regulate affiliative communication. Peripheral administration of the MOR agonist fentanyl increased affiliative singing and calling behavior while reducing stress-related behavior, beak wiping. The effects on vocal but not stress-related behavior were prevented by administration of the NMDA receptor antagonist MK-801. c-Fos mapping revealed that fentanyl increased neural activity in caudal MPOA (cMPOA) and interconnected regions implicated in social behavior, song production, and reward, and that these effects were reversed by MK-801. To identify a local site of MOR-glutamate interaction, we used AAV shRNA to downregulate Shank2 in MPOA. This manipulation prevented fentanyl from stimulating affiliative singing behavior, also without affecting stress reduction, suggesting that MOR–glutamate interactions in the MPOA facilitate social communication but not associated stress reduction. Together these findings provide the first experimental evidence that

JNeurosci Accepted Manuscript

MOR–glutamate interactions within the MPOA, particularly the cMPOA, contribute to affiliative, rewarding vocal communication.

Significance Statement

Affiliative, non-sexual vocal communication is fundamental to social cohesion and well-being, yet its neural mechanisms are poorly understood. This study identifies a critical role for interactions between mu opioid receptors and glutamatergic signaling in promoting non-sexual, rewarding vocal communication. In a songbird experimental system, we demonstrate that NMDA receptor activity and the postsynaptic glutamate receptor scaffolding protein Shank2 are required for opioid facilitation of affiliative song. Our findings further reveal the medial preoptic area, particularly its caudal subdivision, to be an important site of this opioid-glutamate interaction. Together, these results extend opioid–glutamate interaction frameworks beyond classic reward circuits and suggest the existence of a conserved neural mechanism supporting affiliative social behavior across vertebrates.

JNeurosci Accepted Manuscript

Introduction

Affiliative, non-sexual social interactions are essential for the formation and maintenance of social bonds and the acquisition of skills necessary for future social interactions. For example, social play in young animals is critical for the development of adult social skills (Vanderschuren et al., 2016), and vocal-social interactions in non-breeding songbirds play a role in flock cohesion and the development of songs needed to compete for mates and to defend territories in later breeding contexts (Riters et al., 2017; Riters and Stevenson, 2022b). Despite their importance, the mechanisms that underlie affiliative social behaviors outside of reproductive contexts remain poorly understood.

European starlings, *Sturnus vulgaris*, provide a highly tractable system for identifying mechanisms that underlie affiliative social behavior. In addition to the well-studied breeding context, starlings sing at high rates in flocks in non-reproductive contexts, a type of singing behavior that we refer to here as *affiliative*. Affiliative song is produced under low stress conditions, facilitated by the presence of flock mates, and considered important for song learning and flock cohesion (Riters et al., 2017; Maksimoski et al., 2025). Conditioned place preference (CPP) tests demonstrate that birds develop strong preferences for places that they associate with their own production of affiliative song, indicating that the act of producing this type of song is tightly associated with a positive, rewarding affective state (Riters et al., 2014; Hahn et al., 2017; Stevenson et al., 2020).

A strong body of research demonstrates a causal role for mu opioid receptors (MORs) in the medial preoptic area (MPOA) in the production of affiliative song and

JNeurosci Accepted Manuscript

song-associated CPP (Stevenson et al., 2020; Polzin et al., 2022; Riters et al., 2022; Riters and Stevenson, 2022a) that differs from their role in sexually-motivated/courtship song (Stevenson et al., 2020). Recent RNAseq studies also revealed a strong positive association between affiliative song and the expression of a group of glutamatergic co-expressing genes in the MPOA, with the strongest correlations observed for Shank2 (encodes a glutamate receptor scaffolding protein) and GRIN1 (encodes NMDA receptor subunit 1) (Polzin et al., 2023).

These genes form a complex of interacting postsynaptic signaling proteins implicated in social deficits in autistic humans and rodent models of autism spectrum disorder (ASD; (Carlson, 2012; Rojas, 2014; Kim et al., 2019; Montanari et al., 2022)). Shank2 mutations are associated with ASD (Zaslavsky et al., 2019) and Shank2 knockout mice are studied as a model for ASD (Won et al., 2012; Eltokhi et al., 2018; Jung and Park, 2022). Activation of NMDA receptors restores social deficits in Shank2 knockout mice (Won et al., 2012; Gao et al., 2013; Eltokhi et al., 2018), and in at least one study activation of the MPOA reversed social behavior deficits in Shank2 knockout mice (Grabrucker et al., 2021), supporting the hypothesis that in addition to MORs, glutamate action in MPOA contributes to social behavior.

Prior studies on rodents demonstrate that MOR induction of reward depends upon glutamatergic transmission (Popik et al., 2003; Dallimore et al., 2006; Chartoff and Connery, 2014); however, a role for MOR-glutamate interactions in rewarding social behavior has not been explored. Moreover, neural sites of MOR-glutamate interaction explored to date include classic reward sites (i.e., the ventral tegmental area and nucleus accumbens) (Chartoff and Connery, 2014), yet the RNAseq data introduced

JNeurosci Accepted Manuscript

above in starlings suggest the MPOA may also play an essential role. Prior research on another affiliative, rewarding social behavior, social play in rats, also supports a potential role for MOR-glutamate interaction in MPOA in rewarding social behavior with shRNA knockdown of MOR in MPOA found to alter expression of glutamate-related genes and to suppress social play (Zhao et al., 2020). Together, these findings lead to the hypothesis that MOR–glutamate interactions within the MPOA are required for the production of rewarding, non-sexual social behaviors. In this study, we used the unique social communication properties of European starlings to begin to test this hypothesis.

Materials and Methods

Adult European starlings *Sturnus vulgaris* were trapped in winter on a local farm in Madison Wisconsin and housed in mixed-sex flocks in standard cages (0.47 m x 0.47 m x 0.91 m) on a photoperiod of 18h light:6h dark for at least 6 weeks to induce a state of "photorefractoriness," a physiological condition typical of the fall non-breeding season when starlings form flocks, sing high rates of affiliative song, and show no signs of courtship or other reproductive behaviors (Eens, 1997; Riters et al., 2000). All procedures followed protocols approved by the University of Wisconsin Madison Institutional Animal Care and Use Committee and were in accordance with guidelines of the National Institutes of Health.

Experiment 1: Effects of NMDA receptor antagonism on fentanyl-induced affiliative song and potential sites of action

Experiment 1 was designed to determine the contribution of NMDA receptors to MOR-induced song and to identify whether the MPOA is a potential site of action. To

JNeurosci Accepted Manuscript

do this, we examined the effects of the NMDA receptor antagonist MK-801 on the ability of the MOR agonist fentanyl to stimulate song (1A) and used c-Fos immunolabeling as an indirect marker to identify the degree to which MOR and NMDA receptor manipulations altered activity in MPOA, as well as other brain regions (1B).

1A: Pharmacological manipulations and behavior

Experimental Design

For Experiment 1A, experimental birds were housed and tested in one of four flocks consisting of 6 males (including the experimental males) and 2 females in each flock. Each bird was assigned a unique combination of colored leg bands for individual identification. The four flocks were housed separately in indoor aviaries (dimensions: 2.13 m × 2.4 m × 1.98 m) and maintained on an 18h light:6h dark photoperiod. Sports radio was played during lights on to habituate the birds to extraneous noise. Each aviary contained a combination of natural and artificial perches, and birds had ad libitum access to food, drinking water, and bathing water. Treats (e.g., dried crickets) were provided regularly. Flocks were observed for 30 min every other day until birds began to sing. The highest singers from each flock were selected as experimental birds. After they were tested the next highest four singers were tested such that a total of 8 males were tested (in 4 different flocks; 3 birds from flock A, 2 from flock B, 2 from flock C and 1 from flock D). All experimental birds were male because although female starlings sing, they sang less than males.

We then examined the effects of the NMDA receptor antagonist MK-801 on the ability of the MOR agonist fentanyl to stimulate song. Each experimental bird was injected and tested at the same time each day between 10:00 and 12:00 on 4 days

JNeurosci Accepted Manuscript

separated by one day. On each test day birds received one of four subcutaneous injection combinations that included a first injection of Saline or MK-801 (Tocris, Cat. #0924) followed 30 minutes later by administration of Saline or Fentanyl (Sigma-Aldrich, Cat. #F3886) into the inguinal leg fold in counterbalanced order. The injection combinations included 1) Saline + Saline, 2) Saline + Fentanyl (0.25 mg/kg), 3) MK-801 (0.05 mg/kg) + Fentanyl (0.25 mg/kg), and 4) MK-801 (0.1 mg/kg) + Fentanyl (0.25 mg/kg). We selected the MK-801 doses 0.05 and 0.10 mg/kg based on prior studies in birds that indicate these doses to be in the range of effective doses that do not induce motor impairments (Riters and Bingman, 1994; Aamodt et al., 1996). MK-801 and Fentanyl were dissolved in 0.9% saline. The volume for all injections was 0.05 ml. A dose of 0.25 mg/kg fentanyl was used as prior studies show this dose to strongly stimulate affiliative singing behavior in starlings (Stevenson et al., 2020).

Following injections, birds were returned to the aviary with their flock mates. Fifteen minutes after fentanyl injections, bird behaviors were recorded for 15 minutes by an experimenter behind a blind with an iPad camera (iPad mini, Apple). To facilitate social interactions, prior to each observation period dried crickets were placed in the room and if no birds in the focal or neighboring aviaries were singing, recordings of starling song were played for 5 min to facilitate song. Behaviors were manually scored from the videos using the behavior logging software BORIS (Friard and Gamba, 2016). The following behaviors were quantified from recordings: song bouts, time spent singing, calls, beak wipes (considered an indicator of stress), displacement of other birds, preening, flying and hopping as in past studies (Stevenson et al., 2020; Maksimoski et al., 2021; Polzin et al., 2022). Behavior was recorded and coded by a

JNeurosci Accepted Manuscript

single observer who was blind to treatment conditions and data analyzed as detailed in the results section.

1B: Effects of MK-801 and fentanyl manipulations on c-Fos labeling

Experimental Design

After completion of Experiment 1A, in a separate set of 18 males we examined c-Fos immunolabeling as a marker of neuronal activity in MPOA and other brain regions. Birds were selected randomly from 4 standard housing cages that contained 4-5 males and assigned to one of three groups that received either Saline + Saline (n = 6), Saline + Fentanyl (0.25 mg/kg, n = 6) or MK-801 (0.10 mg/kg) + Fentanyl (0.25 mg/kg, n = 6). The injection procedure was the same as Experiment 1. After the second injection, the birds were placed singly into a covered bird cage for 90 min. None of the birds was observed to sing during this time. Birds were then transcardially perfused with 4% paraformaldehyde in 0.1 M phosphate buffer as previously described (Asogwa et al., 2023; Zhao and Riters, 2023). Brains were extracted, postfixed and then cryoprotected in 30% sucrose at 4 °C. Coronal sections (40 µm) were stored at −20 °C until processing.

c-Fos immunohistochemistry using the TSA Biotin System

c-Fos immunolabeling was performed based on previously published protocols with slight modifications (Zhao and Li, 2010; Zhao et al., 2020). All procedures were conducted at room temperature unless otherwise indicated. Brain sections were first washed 5×5 min in 0.02 M phosphate-buffered saline (PBS) to remove cryoprotectant, then incubated in 1.5% H_2O_2 in 50% methanol for 30 min to inhibit endogenous

JNeurosci Accepted Manuscript

peroxidase activity and enhance antibody penetration. Sections were rinsed 3×10 min in PBS containing 0.3% Triton X-100 and 0.05% normal goat serum (NGS), followed by a 60-min incubation in blocking solution (10% NGS, 0.3% Triton X-100 in 0.02 M PBS). Sections were then incubated at 4 °C for 48 h with mouse anti-c-Fos antiserum (E-8; Santa Cruz Biotechnology, sc-166940; 1:1000) diluted in primary antibody incubation solution (PAIS; 0.3% Triton X-100, 1% NGS, 1% blocking reagent in 0.02 M PBS). After primary antibody incubation, sections were washed in TBST (0.05% Tween-20, 0.15 M NaCl, 0.1 M Tris-HCl, pH 7.5) and incubated for 1 h with HRP-conjugated horse anti-mouse antiserum (Cell Signaling Technology, #7076; 1:100). Sections were then washed 3×10 min in TBST and incubated for 30 min in biotinylated tyramide (TSA Biotin System, Akoya Biosciences, NEL700A001KT; 1:100). Following three additional washes in TBST, sections were incubated for 1 h in avidin–biotin complex solution (Vectastain Elite ABC kit, Vector Laboratories, PK-6100; 1:400). After further washes (3×10 min in TBST), immunoreactivity was visualized using diaminobenzidine (DAB; Sigma-Aldrich, D4418) containing 0.008% of $NiCl_2$. Sections were subsequently washed, mounted onto subbed slides, and coverslipped with Serva DePeX. The antibody was validated in starlings using Western blots, and omission of the primary antibody or HRP-conjugated secondary antibody, abolished all specific labeling.

Quantification of c-Fos immunoreactive cells

All images were acquired with a Leica DFC 310 FX digital camera furnished with a Nikon Eclipse E600 microscope using x20 objective lens. Counting of c-Fos immunolabeled cells was performed in the rostral (rMPOA), intermediate (iMPOA),

JNeurosci Accepted Manuscript

and caudal (cMPOA) portions of the medial preoptic area, respectively, in song control regions (Area X and HVC), regions implicated in motivation and reward (nucleus accumbens rostral pole (rNAc), nucleus accumbens shell (sNAc), nucleus accumbens core (cNAc) and the ventral tegmental area (VTA)), and other regions implicated in social behavior (medial bed nucleus of the stria terminalis (BSTm), hippocampal formation (HP), lateral hypothalamus (LHy), lateral septum (LS), periaqueductal gray (PAG), paraventricular nucleus of the hypothalamus (PVN), ventromedial nucleus of the hypothalamus (VMH) (Fig. 1). We note that the NAc has not been well-studied in songbirds. Subregions were selected based on putative NAc locations previously identified in birds (e.g., (Carrillo and Doupe, 2004; Reiner et al., 2004; Balint and Csillag, 2007; Balint et al., 2011; Husband and Shimizu, 2011; Gutierrez-Ibanez et al., 2016)) and evidence in starlings that these sites are immunohistochemically and neuroanatomically similar to mammalian subregions of NAc (Polzin et al., 2021; Polzin et al., 2022). In each bird, the number of c-Fos immunolabeled cells was counted unilaterally in two typical sections that were anatomically well-matched across all animals. Automated cell counting was performed within 450 μm x 450 μm unit area of each interest region by an experimenter unaware of the animal conditions using ImageJ (National Institutes of Health, Bethesda, MD, USA). Cell counts were obtained by subtracting background, applying a threshold that identified labeled cells, applying the watershed function to separate adjacent cells, and analyzing particles. Only cells exhibiting distinct nuclear c-Fos immunoreactivity above background levels were included in the analysis.

JNeurosci Accepted Manuscript

Experiment 2: Effects of Shank2 downregulation in the MPOA on fentanyl-induced affiliative song

Experiment 2 was designed to experimentally test the role of opioid-glutamate interactions specifically in the MPOA. To do this, we examined the effects of shRNA infusions targeting the MPOA on the ability of peripheral fentanyl to stimulate song.

Experimental Design

Twenty-six experimental birds were trapped and housed in standard cages as in Experiment 1. Experimental birds received bilateral infusions of AAV9-GFP-Shank2-shRNA to downregulate Shank2 in the MPOA (n=14). The control condition included surgical controls (n=2; birds that received surgery but no AAV or control infusion) and unmanipulated controls (n= 10). Due to an error, data for an AAV scrambled control group are not available. Therefore, to address possible concerns related to the degree to which differences between AAV treated and control birds were caused by potential damage to the MPOA rather than Shank2 downregulation we included measurement of NeuN.

shRNA design and microinjections of AAV vectors into the MPOA

Target AAV vectors (i.e., AAV9-GFP-U6-Shank2-shRNA) were designed and produced by VectorBuilder (Chicago, USA). We used a cocktail of shRNAs (i.e. a mixture of three different shRNAs) directed toward zebra finch Shank2 gene to improve knockdown efficiency. The shRNA sequences of Shank2 #1 were 5′-CTCCAACAGATGCAGAATAATCTCGAGATTATTCTGCATCTGTTGGAG-TTTTT−3′,

JNeurosci Accepted Manuscript

targeting sequence of CTCCAACAGATGCAGAATAAT of the Shank2 gene. The shRNA sequences of Shank2 #2 were 5′-GCTTCAAGTGACTGCATAATACTCGAGTATTATGCAGTCACTTGAAGC-TTTTT−3′, targeting sequence of GCTTCAAGTGACTGCATAATA of the Shank2 gene. The shRNA sequences of Shank2 #3 were 5′-CTC CAGAGTGGCAACTATAAACTCGAGTTTATAGTTGCCACTCTGGAG-TTTTT−3′, targeting sequence of CTCCAGAGTGGCAACTATAAA of the Shank2 gene. The designed three sets of shRNAs targeted distinct sequences within the coding regions shared by the two Shank2 transcript variants. Transcription of the Shank2 shRNA was driven by a U6 promoter, while the reporter gene, green fluorescent protein (GFP) was driven by a CMV promoter. The sequence between the Shank2 shRNA sequence and the GFP-coding sequence includes a transcription termination sequence (5′-GAATTCCAACTTTGTATAGAAAAGTTG-3′) and the CMV promoter. We note that as in many studies, the CMV promoter driving GFP expression in the Shank2 shRNA AAV vectors is not neuron-specific and can drive gene expression in multiple cell types, including neurons and glial cells. The titers of the three packaged viruses were 2.49×10^{13} GC/ml for ShRNA#1, 1.89×10^{13} GC/ml for ShRNA #2, 1.54×10^{13} GC/ml for ShRNA #3. We followed stereotaxic procedures for microinjection of siRNA into the MPOA of European starling brain (Stevenson et al., 2020). Male birds were securely placed on a stereotaxic apparatus (David Kopf Instruments, Tujunga, California) and anesthetized with isoflurane at vaporizer setting of 2%. A midline anterior to posterior incision was made. Then, the rostral/caudal zero point was determined and cannula (PlasticsOne, 33GA, Roanoke, VA) tip was moved to the coordinates of target site.

JNeurosci Accepted Manuscript

The horizontal coordinate was set at −0.5 mm from skull zero, and the lateral coordinate was positioned at ±0.2 mm from the midline. The AAV vectors expressing Shank2 shRNA (AAV9-GFP-U6-Shank2-shRNA) were injected bilaterally into the MPOA at two sites per hemisphere. The two injection sites were separated by 0.5 mm along the vertical axis, with ventral coordinates of −6.5 mm and −7.0 mm from skull zero. For each injection, 1.0 µl of the AAV vector was administered. After injection, the cannula was left in place for an additional 5 minutes. After recovery, each bird was returned to its home cage.

Behavioral observations

At least 5 weeks after surgery (when shRNA is effective as confirmed through pilot tests), each bird was assigned to one of 6 flocks containing 2 or 3 AAV shRNA-infused experimental birds and 2 unmanipulated control males (focal birds) plus 4 flock mates (2 males and 2 females) that served only as flock stimuli and were not manipulated or observed. We tested 26 birds in total: four birds from each of flocks A, B, C, and D, and five birds from each of flocks E and F. Flocks were housed in indoor aviaries as in Experiment 1. After approximately one week in their new flocks birds were observed singing. Fentanyl manipulations began the following week. One focal bird was tested per day. Each focal bird received saline and fentanyl (0.2 mg/kg) in a counterbalanced order on alternating test days with one day between each test. Note: fentanyl used in this experiment was purchased from a new manufacturer due to back order (Cayman Chemical Company Inc, Ann Arbor, USA; Cat. #22659) and the dose of 0.25 mg/kg chosen in Experiment 1 was too high (after extreme burst of locomotor activity they sat

JNeurosci Accepted Manuscript

still on the floor). We therefore lowered the dose to 0.2 mg/kg and found birds sang at rates similar to those observed in Experiment 1 and did not show motor disturbances. After injection the bird was placed into a small cage for 15 min and then released into the flock. The focal bird was recorded with an iPad for 15 min and behaviors coded as in Experiment 1.

Double immunolabeling for GFP and Shank2 with tyramide signal amplification

Double-label immunohistochemistry was performed on MPOA sections as previously described (Zhao and Gammie, 2015; Merullo et al., 2018; Spool et al., 2018; Zhao et al., 2020). One label targeted GFP to identify neurons transfected by AAV vectors, while the second label targeted Shank2, a protein critical for the regulation of social behavior.

Double-fluorescence immunolabeling was conducted at room temperature unless otherwise specified. Sections were incubated overnight at 4 °C in a mixture of rabbit anti-GFP antiserum (Molecular Probes, A-11122; 1:1000) and mouse anti-Shank2 antiserum (NeuroMab, N23B/6, 75-088; 1:5000). Following primary antibody incubation, sections were incubated for 1 hr with HRP-conjugated horse anti-mouse antiserum (Cell Signaling Technology, No. 7076; 1:100), followed by a 10-min incubation with Cy3-conjugated tyramide (TSA Plus Cyanine 3 kit, PerkinElmer; 1:50) to visualize Shank2 (red). After three washes, sections were incubated for 1 hr with HRP-conjugated goat anti-rabbit antiserum (Cell Signaling Technology, No. 7074; 1:100) and then labeled with Alexa Fluor 488-conjugated tyramide (Alexa Fluor 488 TSA kit, Molecular Probes; 1:100) to visualize GFP (green). Sections were mounted

JNeurosci Accepted Manuscript

on subbed slides, air-dried in the dark for 24 hr, and coverslipped with Serva DePeX. Control procedures, including HRP quenching prior to tyramide incubation or omission of primary or HRP-conjugated secondary antibodies, abolished all specific labeling. The specificity of the Shank2 antibody was also validated by Western blot analysis and by the Shank2 knockdown reported here.

Quantification of Shank2 immunoreactive cells

Images were acquired sequentially at a resolution of 1024 × 1024 pixels using a 20 × objective on an inverted Zeiss LSM 980 confocal microscope equipped with Airyscan 2 (Zeiss; Oberkochen, Germany). For quantitative analysis, the number of single-labeled Shank2 cells was used to assess numbers of Shank2 cells remaining after AAV treatment as compared to controls. Cell counting was performed using 20× magnification photomicrographs in a counting box of 412 µm × 512 µm within the rostral, intermediate and caudal MPOA. In each animal, the number of single-labeled cells was counted bilaterally in a typical section that was anatomically well-matched across all animals (Fig. 1). The counting was performed using Qupath software v0.5.1 (Open software for Bioimage analysis, URL: https://qupath.github.io) by an experienced investigator unaware of the animal conditions. The following parameters were used to identify cells as positive: requested pixel size, 0.5 µm; background radius, 8.0 µm; median filter radius, 4.0 µm; sigma, 1.5 µm; minimum cell area, 10 µm²; maximum cell area, 400 µm²; threshold, 5500; and cell expansion, 5.0 µm. The number of single-labeled Shank2 cells from bilateral MPOA per bird was averaged.

Immunolabeling and quantification of NeuN

JNeurosci Accepted Manuscript

Methods were identical to those described for the c-Fos labeling above except that sections were incubated at 4 °C overnight with mouse anti-NeuN antiserum (MAB377, MilliporeSigma, 1:1000), sections were incubated for 10 min in Cy3-conjugated tyramide, and following three additional washes in TBST, sections were mounted and coverslipped. Control procedures, including omission of the primary antibody or HRP-conjugated secondary antibody, abolished all specific labeling. Images were acquired sequentially and counting performed as described for Shank2.

Statistical Analyses

Behavioral data from Studies 1A and 2 were analyzed in R (v4.6.1; R Foundation for Statistical Computing, Vienna, Austria), and cell-count data were analyzed in GraphPad Prism (v10.1.6; GraphPad Software, San Diego, CA). When assumptions of normality or homogeneity of variance were violated, data were log-transformed prior to analysis.

Behavioral data were analyzed using linear mixed-effects models (lmerTest package) to account for repeated measures of individual birds and potential pseudoreplication arising from testing birds in flocks. In Experiment 1A, treatment (Saline + Saline, Saline + Fentanyl [0.25 mg/kg], MK-801 [0.05 mg/kg] + Fentanyl [0.25 mg/kg], and MK-801 [0.10 mg/kg] + Fentanyl [0.25 mg/kg]) was included as a fixed effect, with bird ID and aviary included as random intercepts. In Experiment 2, drug treatment (saline vs. fentanyl), experimental group (control vs. shRNA), and their interaction were included as fixed effects, with bird ID and aviary included as random intercepts. Fixed effects were evaluated using Type III ANOVA with Satterthwaite approximations for degrees of freedom. Significant effects were followed by post hoc

JNeurosci Accepted Manuscript

pairwise comparisons of estimated marginal means with Tukey-adjusted p values (emmeans package). In Experiment 1B, c-Fos cell counts were analyzed using one-way ANOVA followed by Tukey's post hoc tests, with p values adjusted using the Holm-Bonferroni procedure. In Experiment 2, differences in Shank2 and NeuN cell counts between control and AAV-treated birds were assessed using unpaired t tests with Welch's correction. Correlations were also run to examine associations between Shank2 in MPOA and singing behaviors.

Results

Experiment 1A: MK-801 pretreatment blocked fentanyl-induced affiliative song and other behaviors

Overall effects of MK-801 pretreatment and fentanyl treatment on social behavior

Mixed-effects models revealed significant main effects of treatment conditions on song bouts [$F(3,21) = 12.99$, $p = 0.00005$], time singing [$F(3,21) = 10.63$, $p = 0.0002$], calls [$F(3,21) = 17.26$, $p = 0.000007$], beak wipes [$F(3,25.27) = 9.62$, $p = 0.0002$], preening [$F(3,21) = 4.10$, $p = 0.0195$], and displacement behavior [$F(3,25.24) = 3.19$, $p = 0.0408$]. No main effects were revealed for flying and hopping (both $p > 0.20$) (Fig. 2).

Effects of fentanyl compared to saline treatment on behaviors

Tukey's post hoc tests for the significant ANOVAs above, revealed that fentanyl significantly increased song bouts ($p < 0.0001$, Fig. 2A) and time singing ($p=0.0002$, Fig. 2B) compared to saline treatment. Fentanyl increased calls ($p = 0.0001$, Fig. 2C), but decreased beak wipes ($p = 0.0033$, Fig. 2D) compared to saline treatment,

JNeurosci Accepted Manuscript

consistent with our previous findings. Fentanyl also increased displacement behavior (p = 0.0251 Fig. 2F).

Effects of pretreatment of MK-801 on fentanyl-induced behaviors

Tukey's post hoc tests for the significant ANOVAs above also revealed that pretreatment of MK-801 dose-dependently attenuated fentanyl-induced increase in song bouts (MK-801-0.10, p=0.0015, Fig. 2A), time singing (MK-801-0.10, p=0.0038, Fig. 2B), and calls (MK-801-0.10, p=0.0001, Fig. 2C) but not displacements ($p > 0.34$ for both doses of MK-801, Fig. 2F). Furthermore, the reversal effect of MK-801 on these behaviors appeared to be restored to the normal level as there was no significant difference between the Saline+Saline and MK-801-0.1+Fentanyl group. In contrast, MK-801 had no significant effect on fentanyl-induced decrease in beak wipes (Fig. 2D).

Experiment 1B: c-Fos was differentially expressed across brain regions in response to MK-801 and fentanyl treatments in non-singing birds

Overall effects of MK-801 pretreatment and fentanyl treatment on c-Fos expression

One-way ANOVAs revealed that, of the sixteen brain regions examined, 11 showed a significant effect [BSTm: $F(2, 15)=28.97$, $p<0.0001$; cMPOA: $F(2, 12)=13.19$, $p=0.0009$; cNAc: $F(2, 13)=56.83$, $p<0.0001$; HP: $F(2, 10)=22.26$, $p=0.0002$; HVC: $F(2, 8)=8.211$, $p=0.0115$; iMPOA: $F(2, 15)=9.93$, $p=0.0018$; LS: $F(2, 12)=27.17$, $p<0.0001$; PAG: $F(2, 15)=6.266$, $p=0.0105$; rNAc: $F(2, 13)=50.86$, $p<0.0001$; sNAc: $F(2, 13)=6.469$, $p=0.0112$; VMH: $F(2, 13)=5.613$, $p=0.0175$]. All 11 ANOVAs were also significant using sequential Holm-Bonferroni corrected p values (Figs. 3 and 4).

JNeurosci Accepted Manuscript

Effects of fentanyl treatment on c-Fos expression

Tukey's post hoc tests for the significant ANOVAs above revealed that in comparison to saline treatment, fentanyl significantly increased c-Fos expression in nine forebrain regions examined, including HVC (p=0.0198, Fig. 4B), rNAc (p<0.0001, Fig. 4C), sNAc (p=0.0085, Fig. 4D), cNAc (p<0.0001, Fig. 4E), BSTm (p<0.0001, Fig. 4F), LS (p=0.0018, Figs. 3D-E, 4G), iMPOA (p=0.0018, Fig. 4I), cMPOA (p=0.0009, Figs. 3A-B, 4J), HP (p=0.005, Fig. 4N),

Effects of MK-801 pretreatment on fentanyl-induced c-Fos expression

Tukey's post hoc tests for the significant ANOVAs above also revealed that pretreatment of MK-801 significantly reduced fentanyl-induced c-Fos increase in the rNAc (p=0.0005, Fig. 4C), cNAc (p=0.0006, Fig. 4E), BSTm (p=0.0001, Fig. 4F), LS (p<0.0001, Figs. 3E-F, 4G), cMPOA (p=0.0079, Figs. 3B-C, 4J) and HP (p=0.002, Fig. 4N), but did not alter fentanyl-induced c-Fos increase in the HVC (p=0.9793, Fig. 4B), sNAc (p=0.2325, Fig. 4D), and iMPOA (p=0.5608, Fig. 4I).

Experiment 2: Downregulation of Shank2 in the MPOA disrupted fentanyl-induced affiliative song

Verification of shRNA-mediated Shank2 gene knockdown in MPOA

We performed double labeling for GFP and Shank2. GFP-positive cells were observed in all three subregions of MPOA of all birds injected with the Shank2 AAV vector (Fig. 5A-C), indicating successful viral delivery and efficient transduction within the MPOA. Although the expression levels varied slightly among birds, GFP-positive cells were largely confined to the MPOA, with minimal or no detectable spread to adjacent or distant brain regions. The location of Shank2 knockdown was limited to

JNeurosci Accepted Manuscript

regions in which GFP-positive cells were identified (Fig. 6), and we note that the cellular location in the cell membrane and cytoplasm in starling tissue matches what is observed in humans and rodents (Kim et al., 2018; Woelfle et al., 2023). Shank2-immunoreactive cells were counted and compared with the control birds.

Unpaired t test with Welch's correction revealed that there was a significant difference between Shank2 shRNA AAV and control birds. The number of Shank2-immunoreactive cells was significantly reduced in the rMPOA [$t(23.9)=3.564$, $p=0.0016$; Figs. 5D,G; 7A], iMPOA [$t(23.45)=2.824$, $p=0.0095$; Figs. 5E,H; 7B] and cMPOA [$t(21.39)=2.993$, $p=0.0068$; Figs. 5F,I; 7C] compared to the control. The average percentage of Shank2 knockdown between shRNA AAV and the control birds was 57.4% in rMPOA, 35.6% in iMPOA and 39.4% in cMPOA.

Effects of fentanyl treatment and Shank2 knockdown on behavior

Singing Behaviors

Analyses of both song bouts (Fig. 8A) and time spent singing (Fig. 8B) revealed significant main effects of fentanyl (song bouts: $F(1,43.42) = 20.75$, $p = 0.00004$; time singing: $F(1,43.55) = 20.39$, $p = 0.00005$), significant main effects of Shank2 knockdown (song bouts: $F(1,43.88) = 7.26$, $p = 0.0099$; time singing: $F(1,44.21) = 6.95$, $p = 0.0115$), and significant fentanyl × knockdown interactions (song bouts: $F(1,43.42) = 7.02$, $p = 0.0112$; time singing: $F(1,43.55) = 6.89$, $p = 0.0119$). Post hoc analyses yielded the same pattern for both song measurements. Fentanyl significantly increased singing in control birds (both $p < 0.0001$) but not in shRNA-treated birds (song bouts: $p = 0.168$; time singing: $p = 0.1712$). Control and shRNA-treated birds did not differ under saline treatment (song bouts: $p = 0.9713$; time singing: $p = 0.9927$),

JNeurosci Accepted Manuscript

whereas fentanyl-treated control birds sang more than fentanyl-treated shRNA birds (song bouts: $p = 0.0005$; time singing: $p = 0.0006$).

Other Behaviors

For calls, beak wipes, and preening, significant main effects of fentanyl were observed (Calls: $F(1,24) = 6.22$, $p = 0.0200$; Beak wipes: $F(1,24) = 16.59$, $p = 0.0004$; Preening: $F(1,24) = 4.57$, $p = 0.0429$), but there were no significant effects for knockdown ($p = 0.1058$, 0.9674, 0.8776, respectively) and the interaction was not significant ($p = 0.7392$, 0.5482, 0.6474, respectively; Fig. 8C, D, E). Displacement, flying, and hopping behavior were not significantly affected by fentanyl, knockdown, or their interaction (all $p > 0.10$) (Fig. 8F, G, H). Because our a priori hypotheses concerned the effects of fentanyl within each treatment group, we conducted planned pairwise comparisons irrespective of the omnibus interaction result. This analysis revealed a nearly significant trend for fentanyl to increase calling more in control ($p = 0.0657$) compared to AAV treated birds ($p = 0.1256$). Fentanyl also significantly suppressed beak wipes in both control ($p = 0.0267$) and shRNA treated birds ($p = 0.0021$) (Fig. 8C,D).

Correlations between vocal behavior and Shank2 in MPOA

Correlations were run to determine the degree to which Shank2 in MPOA related to singing behaviors. Analyses were run only on singing birds treated with fentanyl (as these were the only birds observed to sing) and included both control and AAV shRNA treated birds. Significant positive correlations were found only between Shank2 counts in cMPOA and time spent singing ($r=0.74$, $p=0.014$) (Fig. 9C). No significant correlations were found for rMPOA ($r= .19$, $p=0.603$) or iMPOA ($r= .45$, $p=0.197$) (Fig.

JNeurosci Accepted Manuscript

9A,B), and no significant correlations were found in analyses of the number of song bouts (rMPOA r= -0.17, *p*=0.641; iMPOA r=0.30, *p*=0.402; cMPOA r=0.36, *p*=0.310).

Correlations between other behaviors and Shank2 in MPOA

Correlations were also run to explore possible associations between additional behaviors and Shank2 for each subdivision of MPOA followed by sequential Holm-Bonferroni tests. Few birds in each group were observed to beak wipe or displace other birds so correlations were not run on these behaviors. In brief, there were no significant relationships between Shank2 cell counts in rMPOA, iMPOA, or cMPOA and other behaviors when birds from the control and AAV groups were combined. When categorized by treatment group, a significant positive correlation was observed between Shank2 counts in iMPOA and calls in response to fentanyl in the control group (r=0.78, *p*=0.003) but not the AAV treated group (r= -0.46, *p*=0.100). No other significant correlations were identified for Shank2 (*p*>0.05 in all cases).

Analyses of NeuN

Several analyses of NeuN labeling were run to address possible concerns that effects observed for Shank2 relate to neuronal damage to the MPOA rather than Shank2 downregulation. There were no significant differences in NeuN in control compared to AAV shRNA treated birds for any subdivision of MPOA (rMPOA, t(24) = 0.71, p = 0.485; iMPOA, t(24) = 0.73, p = 0.472; cMPOA, t24 = 0.74, p = 0.466) (Figs. 10, 11). There were no significant correlations found between NeuN and Shank2 in any subdivision of MPOA for control or AAV treated birds (rMPOA, control r = 0.21, AAV r = 0.33, p = 0.257; p = 0.508; iMPOA control r = 0.23, p = 0.473, AAV r = -0.46,

JNeurosci Accepted Manuscript

519 p = 0.100, cMPOA control r = 0.19, p = 0.565, AAV r = 0.29, p = 0.307) (in contrast to
520 negative correlations that would be expected if effects of Shank2 related to tissue
521 damage). In contrast to Shank2, no significant correlations were identified between
522 NeuN in cMPOA and time spent singing in singing birds treated with fentanyl (r = -
523 0.31, p = 0.379) or in iMPOA in calls in response to fentanyl in the control group (r =
524 0.37, p = 0.232).

525 **Discussion**

526 The present findings demonstrate that MOR-mediated facilitation of affiliative,
527 non-sexual communication depends on intact glutamatergic signaling. Both systemic
528 pharmacological blockade of NMDA receptors and targeted disruption of the
529 postsynaptic scaffolding protein Shank2 within the MPOA prevented fentanyl from
530 stimulating affiliative vocal behavior in starlings, without altering its stress-reducing
531 effects. These findings provide the first evidence that MOR-glutamate interactions
532 underlie affiliative, reward-associated vocal communication and identify the MPOA as
533 a key neural substrate.

534 ***NMDA receptor blockade prevents MOR facilitation of affiliative song***

535 We first demonstrate that a high dose of the NMDA receptor antagonist MK-801
536 disrupts the ability of the peripherally administered MOR agonist fentanyl to stimulate
537 affiliative song and calling behavior. This demonstrates that NMDA receptor activation
538 is necessary for MOR activation to facilitate vocal communication in an affiliative, non-
539 sexual context. Consistent with our past studies, birds treated with saline alone did not
540 sing, likely reflecting stress-induced inhibition of affiliative song caused by the capture
541 and injection procedures (Stevenson et al., 2020). The finding that fentanyl restored

JNeurosci Accepted Manuscript

542 singing in this context (in this study and in the Shank2 study below) supports the
543 interpretation that MOR activation counteracts stress-related inhibition of vocal
544 behavior.

545 This idea that opioids facilitate affiliative communication by reducing stress is
546 further supported by the finding that fentanyl also reduced beak wiping, which is
547 considered a displacement or stress-related behavior in starlings, as in prior studies
548 (Stevenson et al., 2020). However, beak wipes were not significantly reversed by MK-
549 801, suggesting that NMDA receptor activity may not be necessary for the stress-
550 reducing effects of fentanyl. This is somewhat consistent with reports that MK-801
551 blocks non-opioid mediated but not MOR-mediated analgesic responses to stress
552 (Marek et al., 1991; Marek et al., 1992), though conflicting findings have been reported
553 (Lipa and Kavaliers, 1990). Fentanyl also increased displacements but had no effects
554 on motor behaviors (flying and hopping) or preening, and pre-treatment with MK-801
555 reduced preening at a high dose but had no other significant effects on these
556 behaviors. These results suggest a selective role for MOR-NMDA receptor
557 interactions in social communication.

558 ***The MPOA may be a site of MOR-NMDA interaction***

559 The same fentanyl treatment that stimulated vocal behaviors while reducing stress-
560 related behaviors also increased numbers of c-Fos labeled cells within the
561 intermediate and caudal subdivisions of the MPOA as well as several interconnected
562 brain regions implicated in social behavior (BSTm, LS, and HP), song production
563 (HVC), and reward (NAc). These elevations in c-Fos were reversed in cMPOA (as well
564 as BSTm, NAc, HP, and LS) at the same dose of MK-801 found to prevent the

JNeurosci Accepted Manuscript

facilitation of song by fentanyl. Notably, in the c-Fos study after pharmacological treatments birds were placed alone into cages and were not observed to sing, indicating that these neural changes cannot be attributed to vocal-motor output. Rather we interpret differences to indicate candidate sites of MOR–NMDA receptor interaction.

With respect to the MPOA, these findings extend prior work that demonstrates a strong correlation between expression of the NMDA receptor gene GRIN1 in MPOA and affiliative song (Polzin et al., 2023). Moreover, the finding that c-Fos was increased by fentanyl and reduced by MK-801 pre-treatment selectively within the cMPOA aligns with studies demonstrating functionally-distinct rostral caudal subdivisions within the avian MPOA. Previous studies on birds indicate that the rMPOA is more important than the cMPOA for the regulation of sexual motivation, including courtship song in starlings; whereas caudal portions have been implicated in copulation (Balthazart et al., 1998; Riters and Ball, 1999; Riters et al., 2004; Balthazart and Ball, 2007). The present results raise the possibility that in addition the cMPOA may contribute selectively to nonsexually-motivated, affiliative song.

Shank2 downregulation in MPOA prevents MOR facilitation of affiliative song

In addition to NMDA receptors, our past research revealed a positive correlation between affiliative song and Shank2 expression (Polzin et al., 2023). Here we found that targeted downregulation of Shank2 within the MPOA prevents fentanyl from facilitating affiliative song, paralleling the effects of systemic NMDA receptor inhibition reported above. These findings further support a role for MOR-glutamate interactions

JNeurosci Accepted Manuscript

588 in affiliative song and provide experimental support for the hypothesis that intact
589 glutamate signaling within the MPOA is required for MOR facilitation of affiliative vocal
590 behavior. The finding that reduction of the Shank2 protein in only a single area
591 centered on the MPOA abolished fentanyl-induced affiliative song is particularly
592 striking given that fentanyl was administered peripherally and therefore acting
593 throughout the brain.

594 As in the MK-801 study, fentanyl increased calls. Stress, as indicated by beak
595 wiping, was also reduced by fentanyl in all birds, indicating that glutamate signaling in
596 MPOA may not be necessary for the stress-reducing effects of fentanyl, similar to
597 what we report above in the MK-801 study. Fentanyl was also found to slightly
598 suppress preening behavior. No effects for fentanyl or Shank2 manipulations were
599 found for displacements, flying or hopping, suggesting a selective role for MOR-
600 glutamate interactions in affiliative vocal behavior.

601 Consistent with our prior research (Polzin et al., 2023), Shank2-positive cell counts
602 within MPOA correlated positively with time spent singing. This relationship was
603 specific to cMPOA matching the pattern observed in the c-Fos data above. These
604 findings further support the conclusion that MOR–glutamate interactions particularly
605 within the caudal subdivision of MPOA may be important for affiliative song. In
606 contrast, NeuN counts were not associated with singing, supporting the interpretation
607 that these effects are not driven by general neuronal density or tissue integrity
608 (discussed further below).

609 It is notable that in both studies fentanyl increased calling behavior in a manner
610 similar to song, and this correlated positively with Shank2 in iMPOA in control but not

JNeurosci Accepted Manuscript

AAV treated birds. This was somewhat unexpected, as calls are functionally distinct from song and have not consistently been linked to positive affective states in our prior work. Although call types were not differentiated here, these findings suggest that MOR activation may broadly enhance social vocal output, potentially extending beyond affiliative song to additional forms of communication. Future studies distinguishing call types and a potential role for iMPOA will be necessary to clarify their functional significance.

Limitations and alternative interpretations

A few limitations must be considered when interpreting the results. First, GFP-positive cells were predominantly localized within the MPOA with minimal spread to adjacent or distant brain regions, yet it is possible that downregulation of Shank2 in areas outside the MPOA to some degree contributed to the effects observed here. Another consideration is the absence of a scramble AAV shRNA or vehicle injection control group. This raises the concern that AAV toxicity or tissue damage from injections may have contributed to behavioral effects. Several lines of evidence argue against this interpretation. 1) Lesions to the MPOA tend to increase non-sexually-motivated song, the opposite of the effects observed in AAV treated birds that we report here (Alger and Riters, 2006; Riters and Stevenson, 2022b), 2) NeuN cell counts did not differ between AAV-treated and untreated birds in the present study, 3) NeuN cell counts did not correlate with Shank2 counts, and 4) time spent singing correlated positively with Shank2 but not NeuN labeled cells in cMPOA. Although NeuN labeling does not provide information about all aspects of neuronal functioning

JNeurosci Accepted Manuscript

633 or signaling, this evidence argues against neuronal loss or nonspecific damage
634 explaining the results reported here.

635 ***Significance of the work***

636 The results of the present study integrate previously separate lines of research on
637 opioids and glutamate in the MPOA and affiliative song to reveal a functional
638 interaction between these systems in social behavior. These findings expand upon
639 prior studies in rodents (Chartoff and Connery, 2014) to show that MOR-glutamate
640 interactions underlie naturally rewarding social behavior in addition to drug-related
641 reward. Moreover, the present study demonstrates a previously unreported role for
642 MOR-glutamate interactions in the MPOA in rewarding behavior in addition to
643 canonical reward sites (i.e., ventral tegmental area and nucleus accumbens) that have
644 been the focus of studies on rodents. Together with prior work showing that
645 shRNA-mediated MOR knockdown in the MPOA alters glutamatergic systems and
646 suppresses affiliative, rewarding social play in rats (Zhao et al., 2020), these results
647 suggest that MOR–glutamate interactions within the MPOA may represent a
648 conserved neural mechanism supporting affiliative, rewarding, non-sexual social
649 communication across vertebrates. Future research is needed to more precisely
650 characterize region specific contributions of MOR-glutamate interaction within the
651 MPOA and additional brain regions, including additional regions identified by c-FOS,
652 to affiliative song and other behaviors.

653 The MPOA has long been known for its role in sexual behavior (Hull and
654 Dominguez, 2006; Zhang et al., 2021). The present findings add to a growing number
655 of studies that also implicate the MPOA in rewarding non-sexual social behaviors;

JNeurosci Accepted Manuscript

however, data to date suggest that although MORs in MPOA regulate behavior in both contexts, the role is not the same (e.g., MORs in MPOA stimulate sexually-motivated and inhibit affiliative communication (Stevenson et al., 2020)), similar to effects on sexual behavior and affiliative social play in rats (Hughes et al., 1987; Achterberg et al., 2019). Future studies are needed to explore these differences.

JNeurosci Accepted Manuscript

References

Aamodt SM, Nordeen EJ, Nordeen KW (1996) Blockade of NMDA receptors during song model exposure impairs song development in juvenile zebra finches. Neurobiol Learn Mem 65:91-98.

Achterberg EJM, van Swieten MMH, Houwing DJ, Trezza V, Vanderschuren LJMJ (2019) Opioid modulation of social play reward in juvenile rats. Neuropharmacology 159:107332.

Alger SJ, Riters LV (2006) Lesions to the medial preoptic nucleus differentially affect singing and nest box-directed behaviors within and outside of the breeding season in European starlings (Sturnus vulgaris). Behav Neurosci 120:1326-1336.

Asogwa CN, Zhao C, Polzin BJ, Maksimoski AN, Heimovics SA, Riters LV (2023) Distinct patterns of activity within columns of the periaqueductal gray are associated with functionally distinct birdsongs. Ann N Y Acad Sci 1530:161-181.

Balint E, Csillag A (2007) Nucleus accumbens subregions: hodological and immunohistochemical study in the domestic chick (Gallus domesticus). Cell Tissue Res 327:221-230.

Balint E, Mezey S, Csillag A (2011) Efferent connections of nucleus accumbens subdivisions of the domestic chicken (Gallus domesticus): an anterograde pathway tracing study. J Comp Neurol 519:2922-2953.

Balthazart J, Ball GF (2007) Topography in the preoptic region: differential regulation of appetitive and consummatory male sexual behaviors. Front Neuroendocrinol 28:161-178.

Balthazart J, Absil P, Gerard M, Appeltants D, Ball GF (1998) Appetitive and consummatory male sexual behavior in Japanese quail are differentially regulated by subregions of the preoptic medial nucleus. J Neurosci 18:6512-6527.

Carlson GC (2012) Glutamate receptor dysfunction and drug targets across models of autism spectrum disorders. Pharmacol Biochem Behav 100:850-854.

Carrillo GD, Doupe AJ (2004) Is the songbird Area X striatal, pallidal, or both? An anatomical study. J Comp Neurol 473:415-437.

Chartoff EH, Connery HS (2014) It's MORe exciting than mu: crosstalk between mu opioid receptors and glutamatergic transmission in the mesolimbic dopamine system. Front Pharmacol 5:116.

Dallimore JE, Mickiewicz AL, Napier TC (2006) Intra-ventral pallidal glutamate antagonists block expression of morphine-induced place preference. Behav Neurosci 120:1103-1114.

Eens M (1997) Understanding the complex song of the European starling: An integrated approach. Adv Study Beh 26:355-434.

Eltokhi A, Rappold G, Sprengel R (2018) Distinct Phenotypes of Shank2 Mouse Models Reflect Neuropsychiatric Spectrum Disorders of Human Patients With SHANK2 Variants. Front Mol Neurosci 11:240.

Friard O, Gamba M (2016) BORIS: a free, versatile open-source event-logging software for video/audio coding and live observations. Methods in ecology and evolution 7:1325-1330.

Gao C, Tronson NC, Radulovic J (2013) Modulation of behavior by scaffolding proteins of the post-synaptic density. Neurobiol Learn Mem 105:3-12.

Grabrucker S, Pagano J, Schweizer J, Urrutia-Ruiz C, Schon M, Thome K, Ehret G, Grabrucker AM, Zhang R, Hengerer B, Bockmann J, Verpelli C, Sala C, Boeckers TM (2021) Activation of the medial preoptic area (MPOA) ameliorates loss of maternal behavior in a Shank2 mouse model for autism. EMBO J 40:e104267.

JNeurosci Accepted Manuscript

Gutierrez-Ibanez C, Iwaniuk AN, Jensen M, Graham DJ, Pogány Á, Mongomery BC, Stafford JL, Luksch H, Wylie DR (2016) Immunohistochemical localization of cocaine- and amphetamine-regulated transcript peptide (CARTp) in the brain of the pigeon (Columba livia) and zebra finch (Taeniopygia guttata). J Comp Neurol 524:3747-3773.

Hahn AH, Merullo DP, Spool JA, Angyal CS, Stevenson SA, Riters LV (2017) Song-associated reward correlates with endocannabinoid-related gene expression in male European starlings (Sturnus vulgaris). Neuroscience 346:255-266.

Hughes AM, Everitt BJ, Herbert J (1987) Selective effects of beta-endorphin infused into the hypothalamus, preoptic area and bed nucleus of the stria terminalis on the sexual and ingestive behaviour of male rats. Neuroscience 23:1063-1073.

Hull EM, Dominguez JM (2006) Getting his act together: roles of glutamate, nitric oxide, and dopamine in the medial preoptic area. Brain Res 1126:66-75.

Husband SA, Shimizu T (2011) Calcium-binding protein distributions and fiber connections of the nucleus accumbens in the pigeon (Columba livia). J Comp Neurol 519:1371-1394.

Jung S, Park M (2022) Shank postsynaptic scaffolding proteins in autism spectrum disorder: Mouse models and their dysfunctions in behaviors, synapses, and molecules. Pharmacol Res 182:106340.

Kim JW, Park K, Kang RJ, Gonzales ELT, Kim DG, Oh HA, Seung H, Ko MJ, Kwon KJ, Kim KC, Lee SH, Chung C, Shin CY (2019) Pharmacological modulation of AMPA receptor rescues social impairments in animal models of autism. Neuropsychopharmacology 44:314-323.

Kim R, Kim J, Chung C, Ha S, Lee S, Lee E, Yoo YE, Kim W, Shin W, Kim E (2018) Cell-Type-Specific Shank2 Deletion in Mice Leads to Differential Synaptic and Behavioral Phenotypes. J Neurosci 38:4076-4092.

Lipa SM, Kavaliers M (1990) Sex differences in the inhibitory effects of the NMDA antagonist, MK-801, on morphine and stress-induced analgesia. Brain Res Bull 24:627-630.

Maksimoski AN, Levenson TA, Zhao C, Riters LV (2025) Evidence that flocking behavior is rewarded by singing, flock mates, and mu opioid receptors in the nucleus accumbens. PLoS One 20:e0318340.

Maksimoski AN, Polzin BJ, Stevenson SA, Zhao C, Riters LV (2021) μ-Opioid Receptor Stimulation in the Nucleus Accumbens Increases Vocal-Social Interactions in Flocking European Starlings,. eNeuro 8.

Marek P, Page GG, Ben-Eliyahu S, Liebeskind JC (1991) N-methyl-D-aspartic acid (NMDA) receptor antagonist MK-801 blocks non-opioid stress-induced analgesia. I. Comparison of opiate receptor-deficient and opiate receptor-rich strains of mice. Brain Res 551:293-296.

Marek P, Mogil JS, Sternberg WF, Panocka I, Liebeskind JC (1992) N-methyl-D-aspartic acid (NMDA) receptor antagonist MK-801 blocks non-opioid stress-induced analgesia. II. Comparison across three swim-stress paradigms in selectively bred mice. Brain Res 578:197-203.

Merullo DP, Spool JA, Zhao C, Riters LV (2018) Co-localization patterns of neurotensin receptor 1 and tyrosine hydroxylase in brain regions involved in motivation and social behavior in male European starlings. J Chem Neuroanat 89:1-10.

Montanari M, Martella G, Bonsi P, Meringolo M (2022) Autism Spectrum Disorder: Focus on Glutamatergic Neurotransmission. Int J Mol Sci 23.

Polzin BJ, Heimovics SA, Riters LV (2021) Immunolabeling Provides Evidence for Subregions in the Songbird Nucleus Accumbens and Suggests a Context-Dependent Role in Song in Male European Starlings (Sturnus vulgaris). Brain Behav Evol 96:147-162.

JNeurosci Accepted Manuscript

761 Polzin BJ, Stevenson SA, Gammie SC, Riters LV (2023) Distinct patterns of gene expression
762 in the medial preoptic area are related to gregarious singing behavior in European
763 starlings (Sturnus vulgaris). BMC Neurosci 24:41.
764 Polzin BJ, Maksimoski AN, Stevenson SA, Zhao C, Riters LV (2022) Mu opioid receptor
765 stimulation in the medial preoptic area or nucleus accumbens facilitates song and
766 reward in flocking European starlings. Front Physiol 13:970920.
767 Popik P, Wrobel M, Rygula R, Bisaga A, Bespalov AY (2003) Effects of memantine, an NMDA
768 receptor antagonist, on place preference conditioned with drug and nondrug
769 reinforcers in mice. Behav Pharmacol 14:237-244.
770 Reiner A et al. (2004) Revised nomenclature for avian telencephalon and some related
771 brainstem nuclei. J Comp Neurol 473:377-414.
772 Riters LV, Bingman VP (1994) The NMDA-receptor antagonist MK-801 impairs navigational
773 learning in homing pigeons. Behav Neural Biol 62:50-59.
774 Riters LV, Ball GF (1999) Lesions to the medial preoptic area affect singing in the male
775 European starling (Sturnus vulgaris). Horm Behav 36:276-286.
776 Riters LV, Stevenson SA (2022a) Using seasonality and birdsong to understand mechanisms
777 underlying context-appropriate shifts in social motivation and reward. Hormones and
778 Behavior 142:1-10.
779 Riters LV, Stevenson SA (2022b) Using seasonality and birdsong to understand mechanisms
780 underlying context-appropriate shifts in social motivation and reward. Horm Behav
781 142:105156.
782 Riters LV, Teague DP, Schroeder MB, Cummings SE (2004) Vocal production in different
783 social contexts relates to variation in immediate early gene immunoreactivity within
784 and outside of the song control system. Behav Brain Res 155:307-318.
785 Riters LV, Stevenson SA, DeVries MS, Cordes MA (2014) Reward associated with singing
786 behavior correlates with opioid-related gene expression in the medial preoptic nucleus
787 in male European starlings. PLoS One 9:e115285.
788 Riters LV, Spool JA, Merullo DP, Hahn AH (2017) Song practice as a rewarding form of play
789 in songbirds. Behav Processes.
790 Riters LV, Polzin BJ, Maksimoski AN, Stevenson SA, Alger SJ (2022) Birdsong and the neural
791 regulation of positive emotion. Front Psychol 13:1-17.
792 Riters LV, Eens M, Pinxten R, Duffy DL, Balthazart J, Ball GF (2000) Seasonal changes in
793 courtship song and the medial preoptic area in male European starlings (Sturnus
794 vulgaris). Horm Behav 38:250-261.
795 Rojas DC (2014) The role of glutamate and its receptors in autism and the use of glutamate
796 receptor antagonists in treatment. J Neural Transm (Vienna) 121:891-905.
797 Spool JA, Merullo DP, Zhao C, Riters LV (2018) Co-localization of mu-opioid and dopamine
798 D1 receptors in the medial preoptic area and bed nucleus of the stria terminalis across
799 seasonal states in male European starlings. Horm Behav.
800 Stevenson SA, Piepenburg A, Spool JA, Angyal CS, Hahn AH, Zhao C, Riters LV (2020)
801 Endogenous opioids facilitate intrinsically-rewarded birdsong. Sci Rep 10:11083.
802 Vanderschuren LJ, Achterberg EJ, Trezza V (2016) The neurobiology of social play and its
803 rewarding value in rats. Neurosci Biobehav Rev 70:86-105.
804 Woelfle S, Pedro MT, Wagner J, Schön M, Boeckers TM (2023) Expression profiles of the
805 autism-related SHANK proteins in the human brain. BMC Biol 21:254.
806 Won H, Lee HR, Gee HY, Mah W, Kim JI, Lee J, Ha S, Chung C, Jung ES, Cho YS, Park SG,
807 Lee JS, Lee K, Kim D, Bae YC, Kaang BK, Lee MG, Kim E (2012) Autistic-like social
808 behaviour in Shank2-mutant mice improved by restoring NMDA receptor function.
809 Nature 486:261-265.
810 Zaslavsky K, Zhang WB, McCready FP, Rodrigues DC, Deneault E, Loo C, Zhao M, Ross PJ,
811 El Hajjar J, Romm A, Thompson T, Piekna A, Wei W, Wang Z, Khattak S, Mufteev M,

JNeurosci Accepted Manuscript

Pasceri P, Scherer SW, Salter MW, Ellis J (2019) SHANK2 mutations associated with autism spectrum disorder cause hyperconnectivity of human neurons. Nat Neurosci 22:556-564.

Zhang SX, Lutas A, Yang S, Diaz A, Fluhr H, Nagel G, Gao S, Andermann ML (2021) Hypothalamic dopamine neurons motivate mating through persistent cAMP signalling. Nature 597:245-249.

Zhao C, Li M (2010) c-Fos identification of neuroanatomical sites associated with haloperidol and clozapine disruption of maternal behavior in the rat. Neuroscience 166:1043-1055.

Zhao C, Gammie SC (2015) Metabotropic glutamate receptor 3 is downregulated and its expression is shifted from neurons to astrocytes in the mouse lateral septum during the postpartum period. J Histochem Cytochem 63:417-426.

Zhao C, Riters LV (2023) The medial preoptic area and its projections to the ventral tegmental area and the periaqueductal gray are activated in response to social play behavior in juvenile rats. Behav Neurosci 137:223-235.

Zhao C, Chang L, Auger AP, Gammie SC, Riters LV (2020) Mu opioid receptors in the medial preoptic area govern social play behavior in adolescent male rats. Genes Brain Behav 19:e12662.

JNeurosci Accepted Manuscript

Figure legends

Figure 1. Brain regions analyze for c-Fos expression in starlings. Illustrations of one hemisphere of coronal starling brain sections. Ovals and circles indicate the regions in which c-Fos expression was examined and quantified. Abbreviations: BSTm, medial bed nucleus of the stria terminalis; cMPOA, caudal portion of the medial preoptic area; cNAc, nucleus accumbens core; HP, hippocampus; HVC, proper name; iMPOA, intermediate portion of the medial preoptic area; LHy, lateral hypothalamus; LS, lateral septum; PAG, periaqueductal gray; PVN, paraventricular nucleus of the hypothalamus; rMPOA, rostral portion of the medial preoptic area; rNAc, nucleus accumbens rostral pole; sNAc, nucleus accumbens shell; VMH, ventromedial nucleus of the hypothalamus; VTA, ventral tegmental area.

Figure 2. Effects of MK-801 on fentanyl-induced behaviors. A) song bouts; B) time singing; C) calls; D) beak wipes; E) preening; F) displacements; G) flying; H) hopping. Data in A-D were log transformed before statistical analysis. The labeling of the x axis in panels F-H applies to those in panels A-E. Each point represents an individual bird. Means and standard errors are indicated. * $p<0.05$, ** $p<0.01$, *** $p< 0.001$, **** $p<0.0001$.

Figure 3. Representative photomicrographs of c-Fos expression in the cMPOA and LS. c-Fos expression was quantified in the cMPOA (boxed areas, A-C) and LS (D-F). Saline+Saline (A,D); Saline+Fentanyl (B,E); MK-801+Fentanyl (C,F). Abbreviations:

JNeurosci Accepted Manuscript

cMPOA, caudal portion of the medial preoptic area; LS, lateral septum. Scale bar: 100 μm in A-C and 50 μm in D-F.

Figure 4. c-Fos identification of neuroanatomical regions implicated in opioid-glutamate interactions associated with affiliative song. c-Fos expression was quantified in 16 brain regions. Data for B-P were log transformed and then statistically analyzed. The labeling of the x axis in panels M-P applies to those in panels A-L. Panels outlined in red indicate candidate brain regions involved in opioid-glutamate interactions that regulate affiliative song. Abbreviations: BSTm, medial bed nucleus of the stria terminalis; cMPOA, caudal portion of the medial preoptic area; cNAc, nucleus accumbens core; HP, hippocampus; HVC, proper name; iMPOA, intermediate portion of the medial preoptic area; LHy, lateral hypothalamus; LS, lateral septum; PAG, periaqueductal gray; PVN, paraventricular nucleus of the hypothalamus; rMPOA, rostral portion of the medial preoptic area; rNAc, nucleus accumbens rostral pole; sNAc, nucleus accumbens shell; VMH, ventromedial nucleus of the hypothalamus; VTA, ventral tegmental area. Each point represents an individual bird. Means and standard errors are indicated. * p<0.05, ** p<0.01, *** p< 0.001, **** p<0.0001.

Figure 5. Verification of viral transduction and Shank2 knockdown in the MPOA. Immunofluorescence labeling for GFP was used as a reporter to identify transduced cells, and immunohistochemical analysis was performed to assess changes in Shank2 expression within the MPOA (white boxed areas). A large number of GFP-positive cells were observed in the rMPOA (A), iMPOA (B), and cMPOA (C), indicating

JNeurosci Accepted Manuscript

successful injection and efficient viral transduction throughout the MPOA. Note that the number of Shank2-immunoreactive cells was significantly reduced in the rMPOA (D and G), iMPOA (E and H) and cMPOA (F and I) in knockdown birds compared to the controls. Arrows indicate typical GFP-positive cells, and arrowheads indicate Shank2-labeled cells. GFP, green fluorescent protein; cMPOA, caudal portion of the medial preoptic area; rMPOA, rostral portion of the medial preoptic area; iMPOA, intermediate portion of the medial preoptic area. Scale bar: 100 μm in A-C and 200 μm in D-I.

Figure 6. Shank2 was depleted in AAV treated birds in areas that contained GFP-positive cells. Representative photomicrographs of cMPOA demonstrating that relative to controls (A-C), numbers of Shank2 labeled cells were reduced (D) in regions in which AAV (as indicated by GFP) was detected (E and F). Scale bar: 100 μm

Figure 7. Quantification of Shank2 knockdown in the MPOA. The Shank2 expression was assessed by counting the number of Shank2 immunoreactive cells. Data in A were log transformed before statistical analysis. The number of Shank2-immunoreactive cells was significantly reduced in the rMPOA (A), iMPOA (B) and cMPOA (C) in knockdown birds compared to the controls. Each point represents an individual bird. Means and standard errors are indicated. ** $p<0.01$.

Figure 8. Shank2 knockdown prevents fentanyl-induced vocal behaviors. A) song bouts; B) time singing; C) calls; D) beak wipes; E) preening; F) displacements; G)

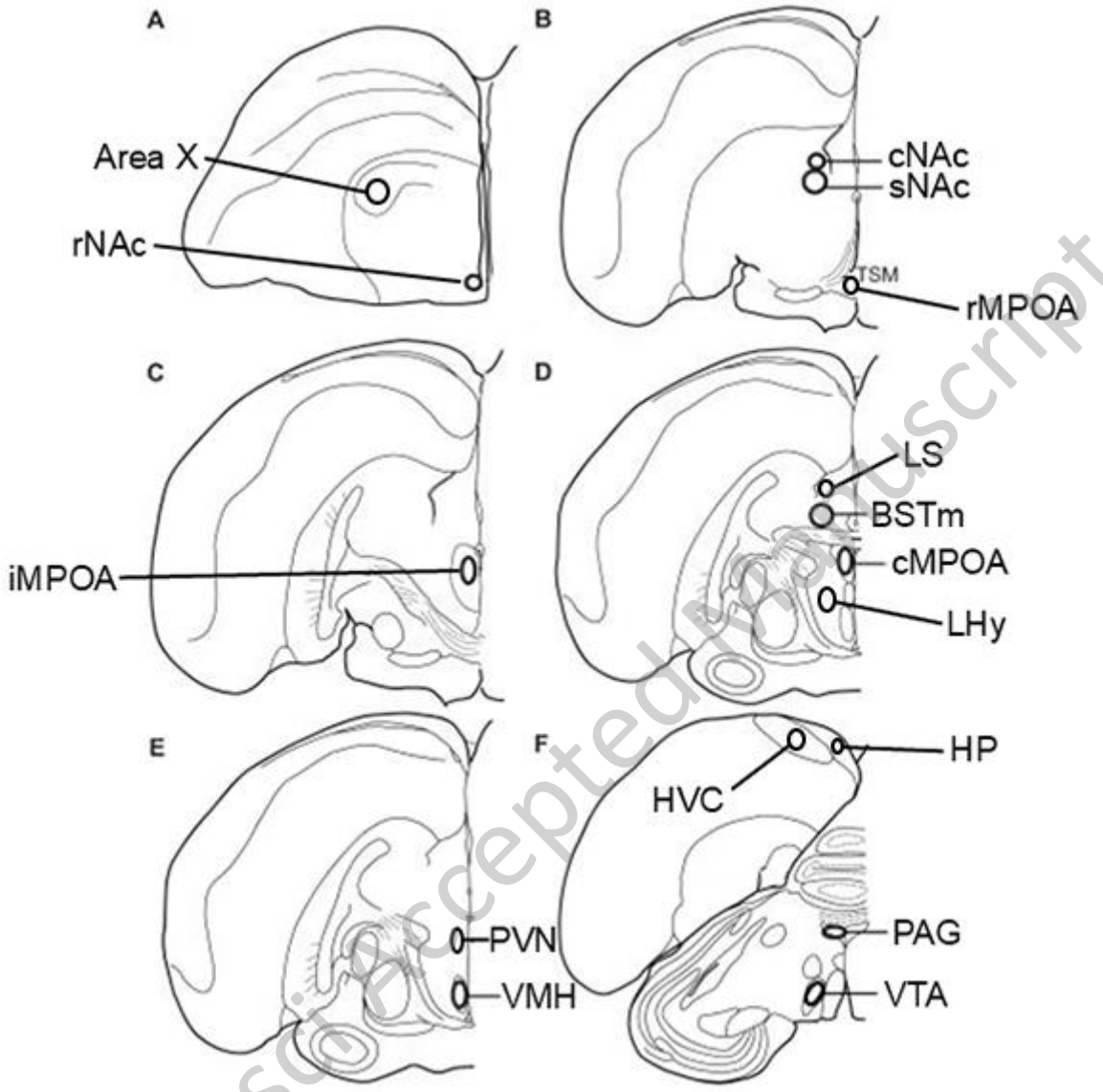
JNeurosci Accepted Manuscript

899 flying; H) hopping. All data were log transformed before statistical analysis. Each point
900 represents an individual bird. Means and standard errors are indicated. * p<0.05, **
901 p<0.01, *** p< 0.001, **** p<0.0001. Significant main effects are reported in Results.
902
903 Figure 9. Shank2-immunoreactive cell counts in cMPOA correlate with time spent
904 singing. Scatterplots illustrating the relationships between the number of Shank2
905 immunolabeled cells in A) rostral portion of the medial preoptic area; rMPOA; B)
906 intermediate portion of the medial preoptic area; iMPOA; and C) caudal portion of the
907 medial preoptic area; cMPOA and time spent singing (in secs) in birds treated with
908 fentanyl (see text for details). Each point represents an individual bird. Regression line
909 indicates a significant correlation p<0.05.
910
911 Figure 10. NeuN immunolabeling in the MPOA of control and Shank2 knockdown
912 birds. Immunohistochemical analysis was performed to quantify NeuN expression
913 within the MPOA (white boxed areas). Representative images are shown for control
914 and Shank2 knockdown birds in the rostral medial preoptic area (rMPOA; A, B),
915 intermediate medial preoptic area (iMPOA; C, D), and caudal medial preoptic area
916 (cMPOA; E, F). Panels G and H show higher-magnification images of the cMPOA.
917 Scale bar, 200 μm in A-F and 100 μm in G-H.
918
919 Figure 11. Quantification of NeuN-immunoreactive cells in the MPOA. Data in B and C
920 were log transformed before statistical analysis. The number of NeuN-immunolabeled
921 cells did not differ between Shank2 knockdown and control birds in the rostral medial

JNeurosci Accepted Manuscript

preoptic area (rMPOA; A), intermediate medial preoptic area (iMPOA; B), or caudal medial preoptic area (cMPOA; C). Each point represents an individual bird. Means and standard errors are indicated.

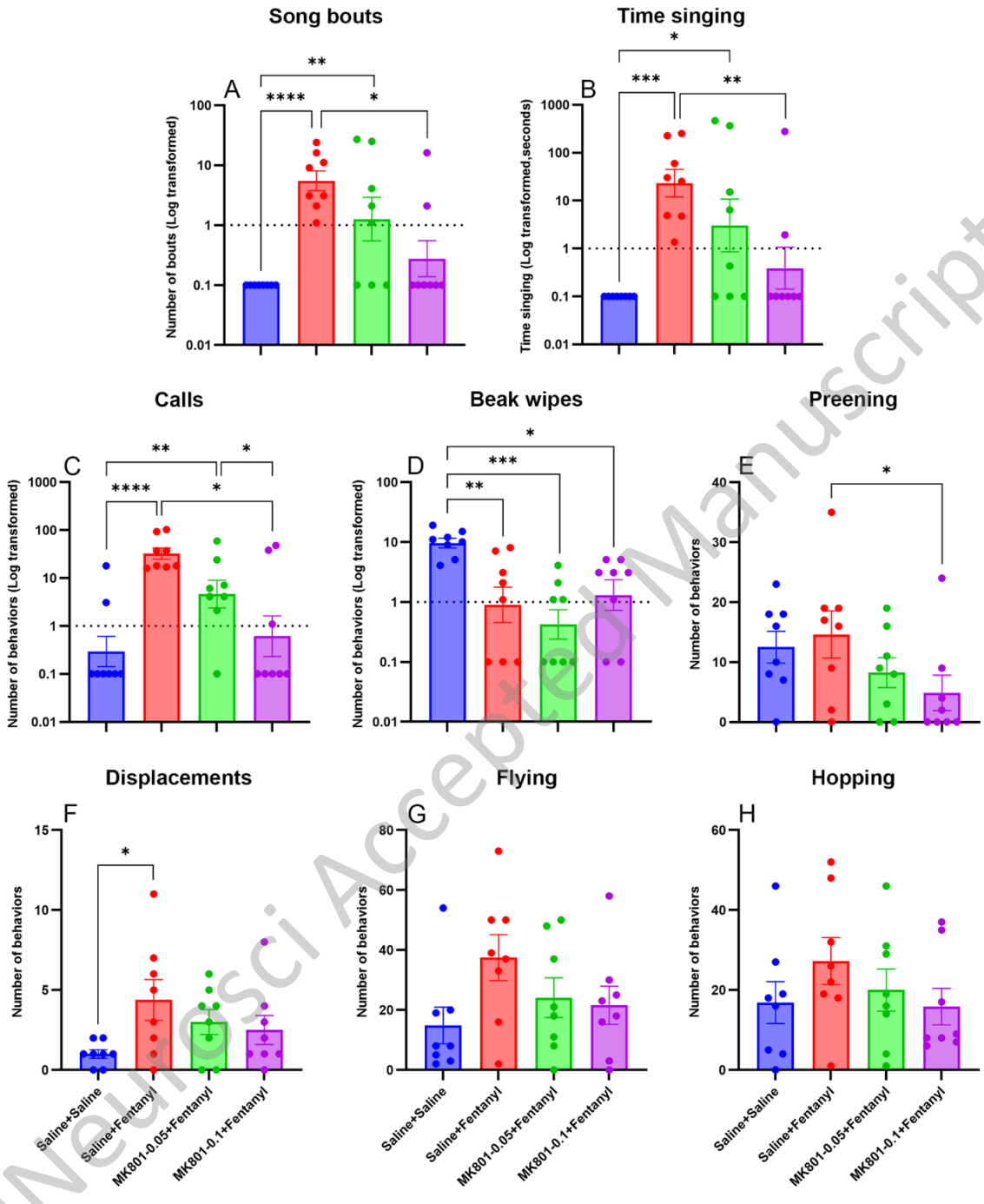
JNeurosci Accepted Manuscript



926

927

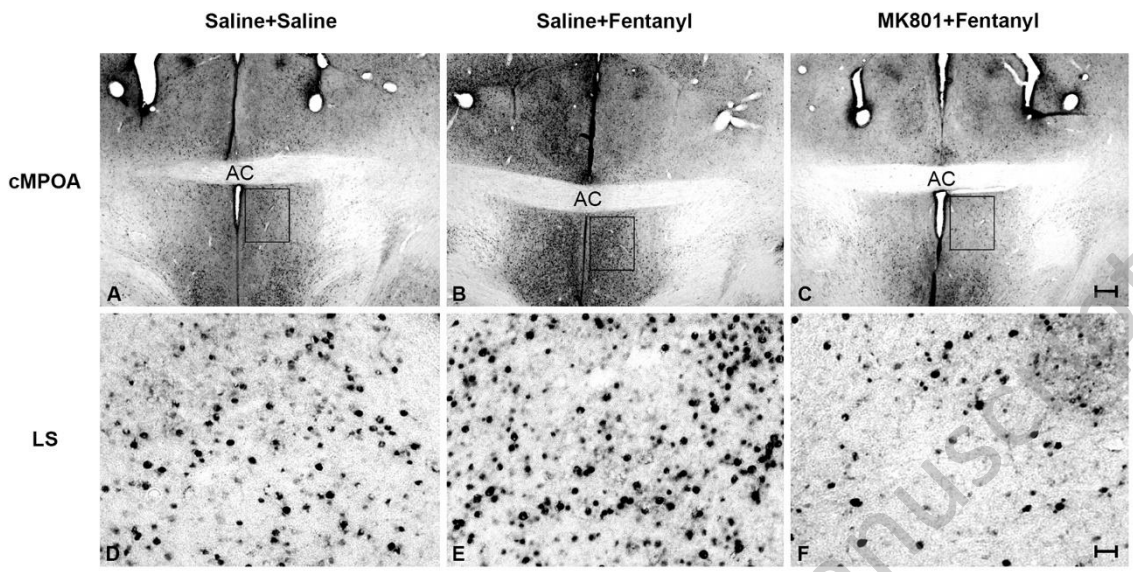
JNeurosci Accepted Manuscript



928

929

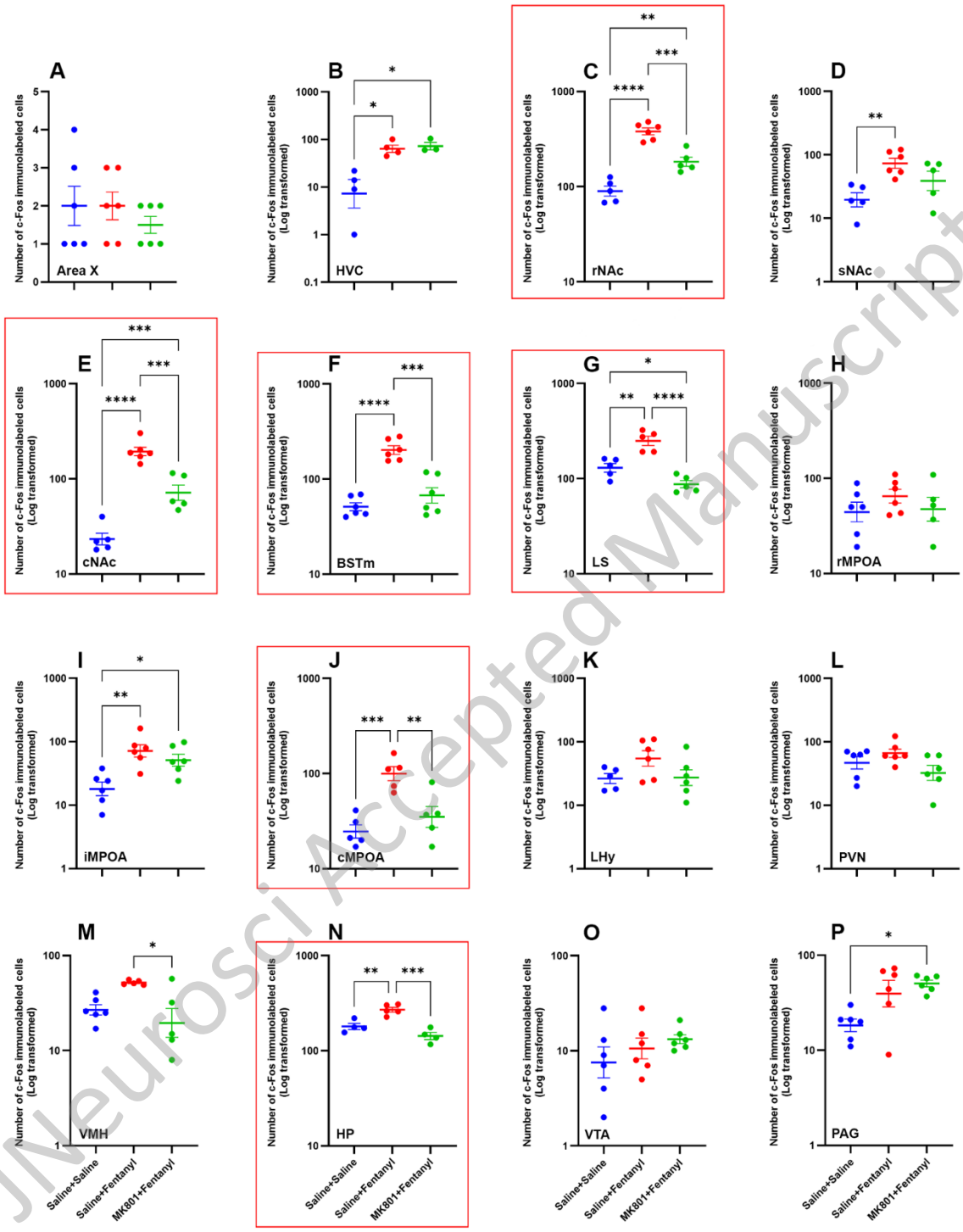
JNeurosci Accepted Manuscript



930

931

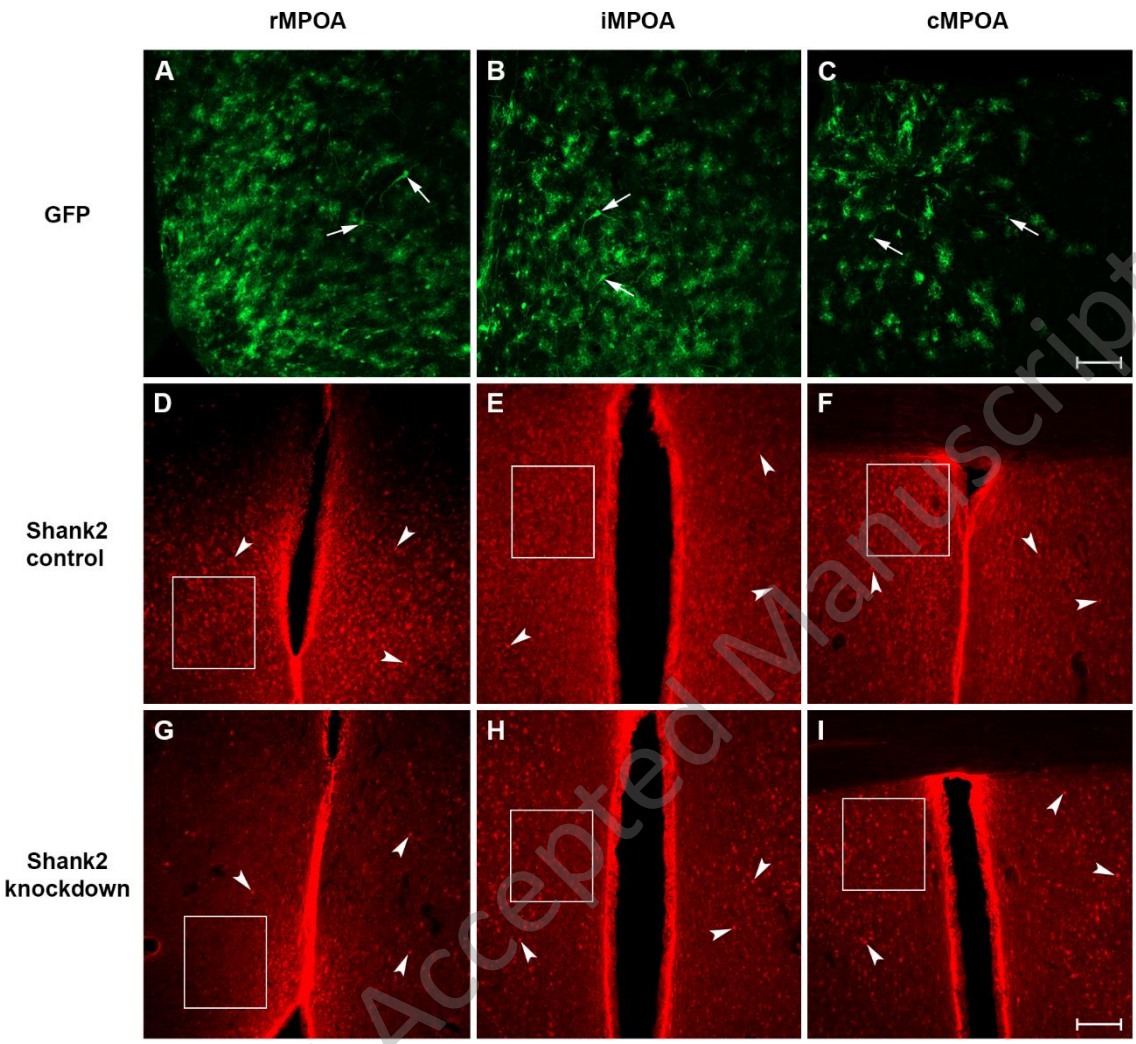
JNeurosci Accepted Manuscript



JNeurosci Accepted Manuscript

932

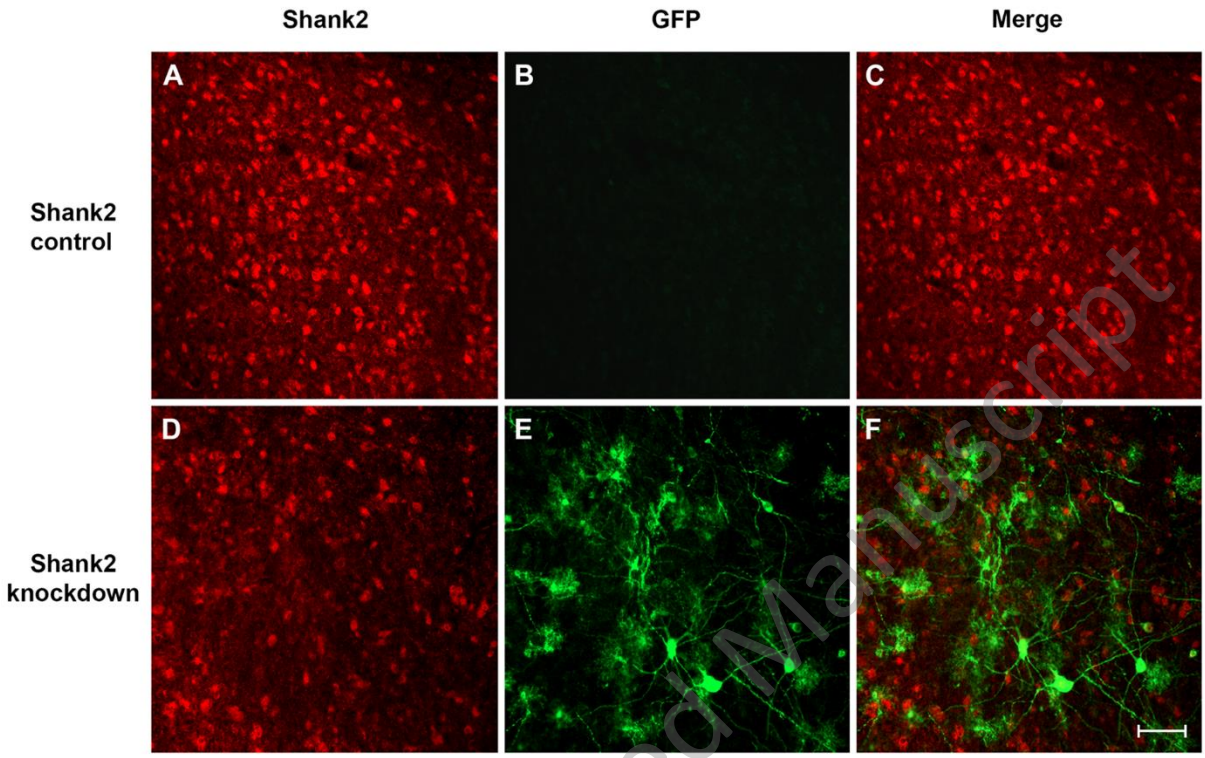
933



934

935

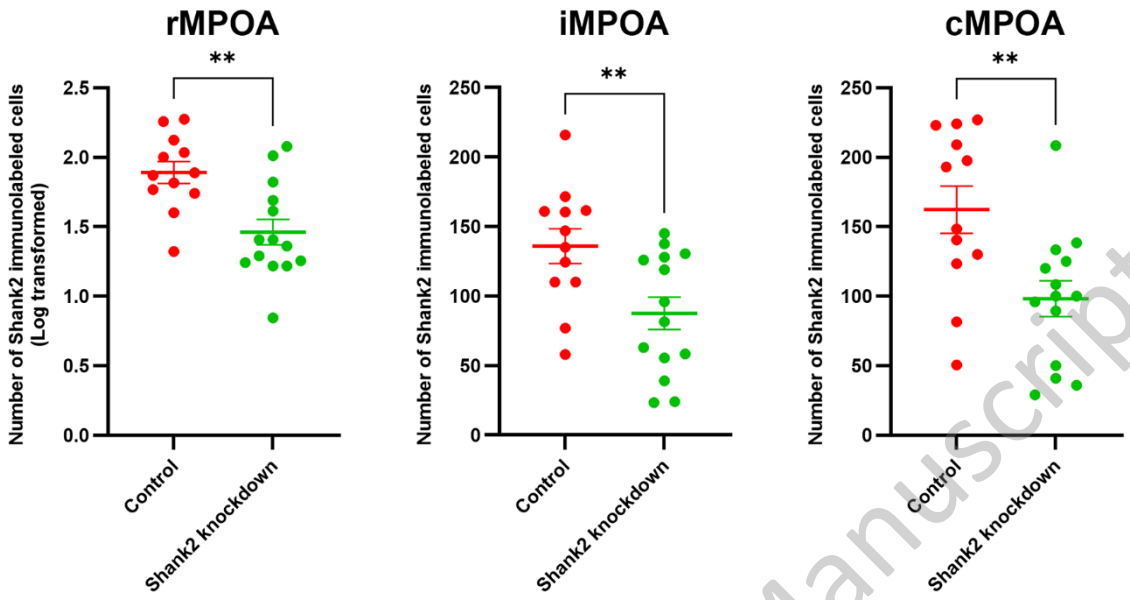
JNeurosci Accepted Manuscript



936

937

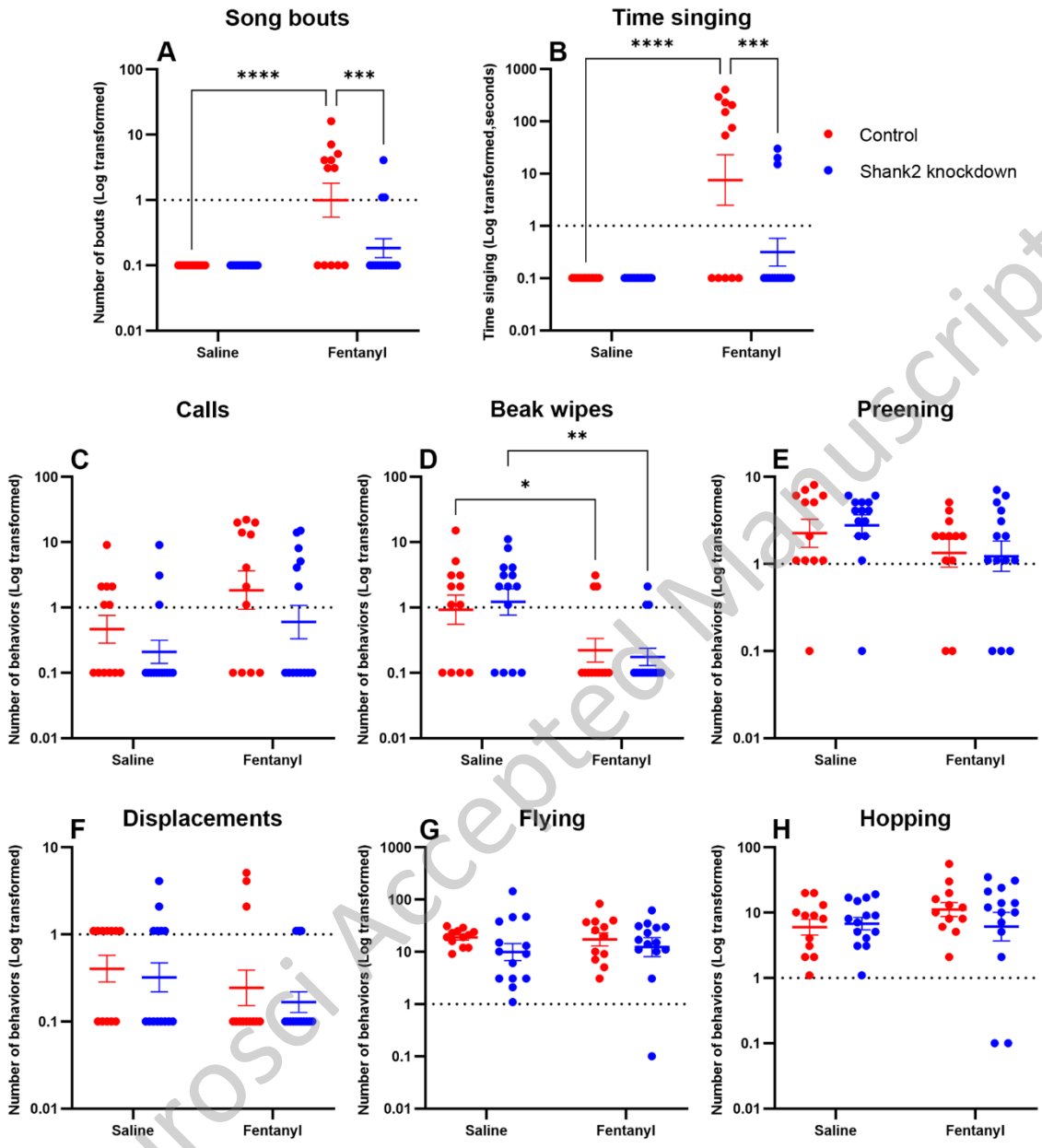
JNeurosci Accepted Manuscript



938

939

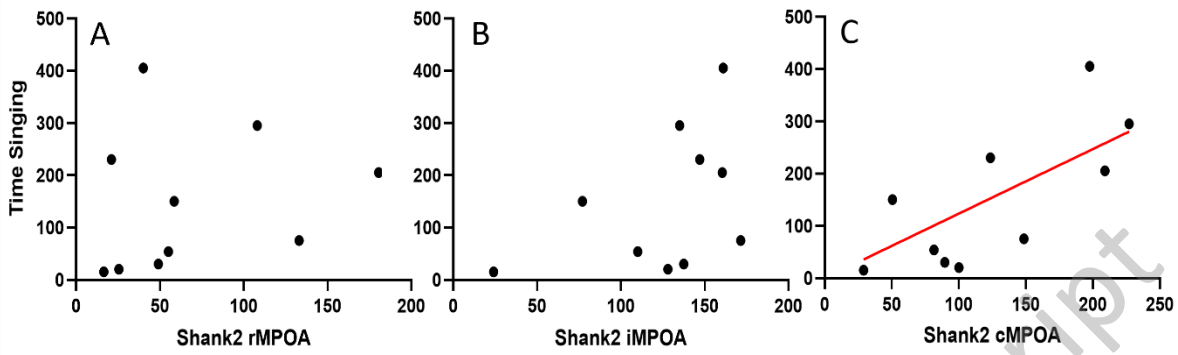
JNeurosci Accepted Manuscript



940

941

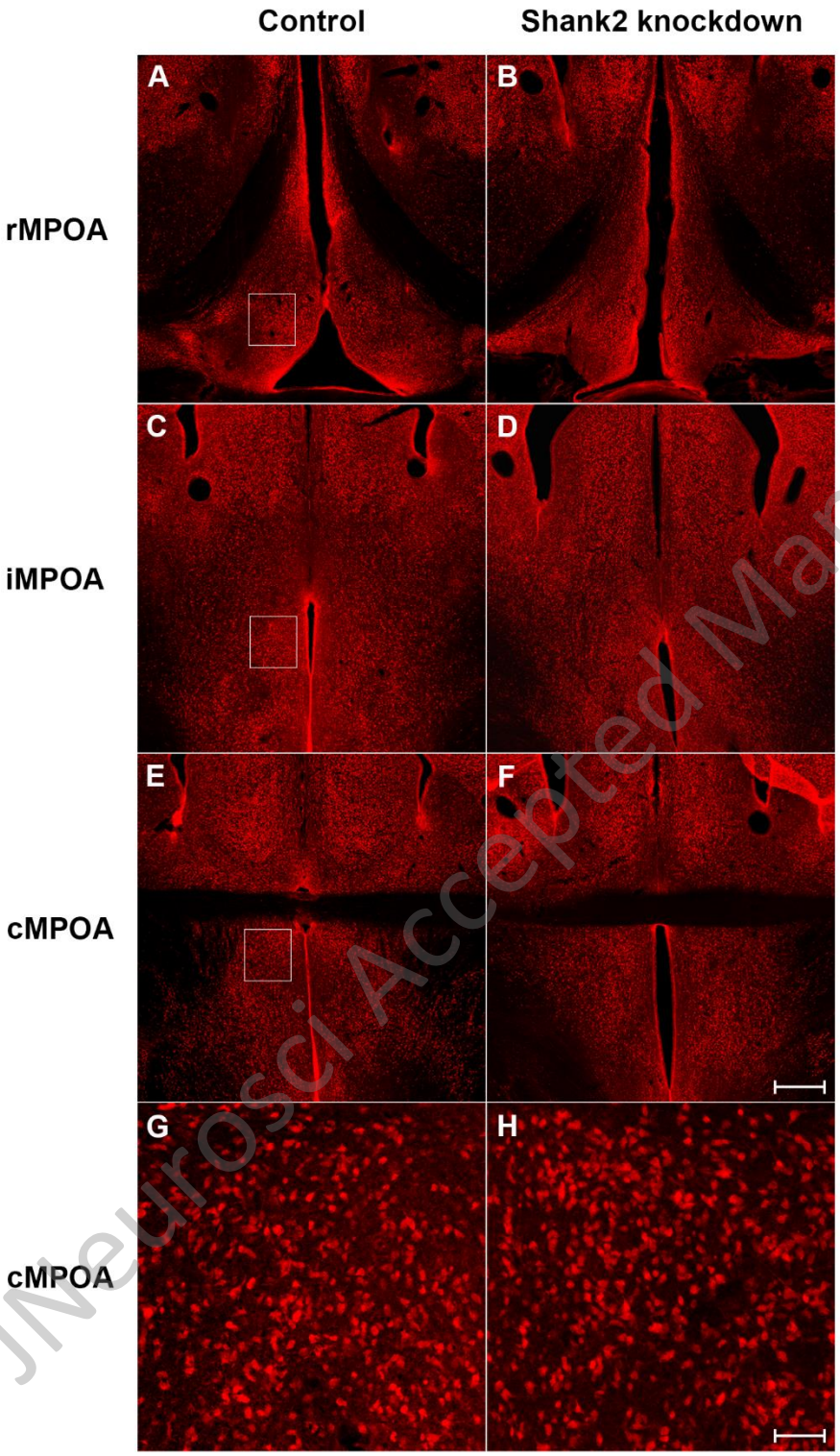
JNeurosci Accepted Manuscript



942

943

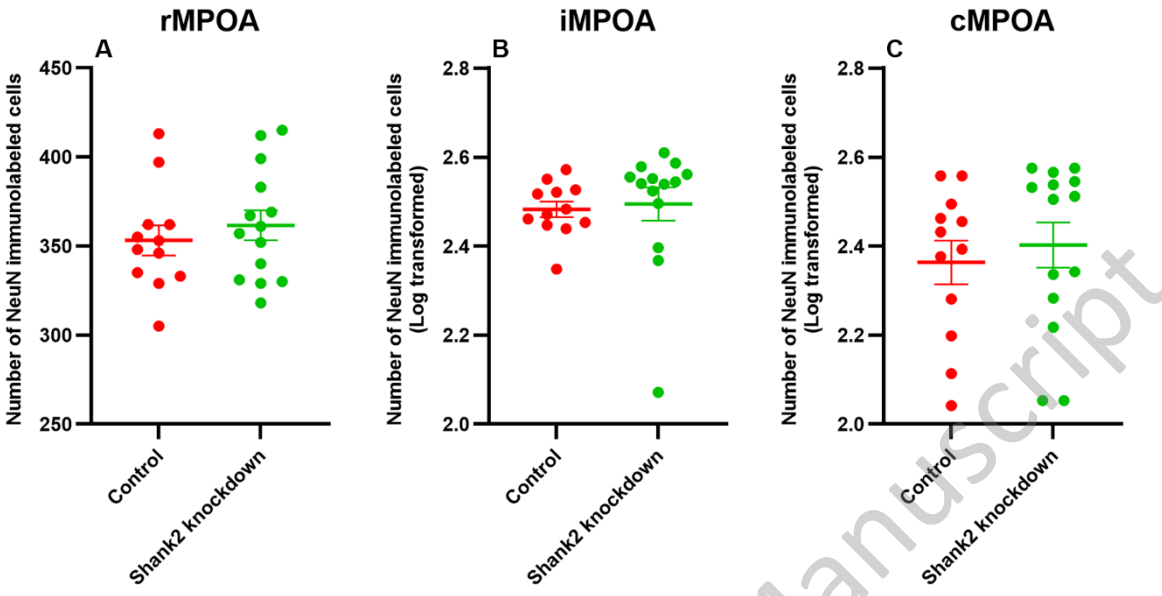
JNeurosci Accepted Manuscript



944

945

JNeurosci Accepted Manuscript



946

JNeurosci Accepted Manuscript